Acta Crystallographica Section B
Structural Science
ISSN 0108-7681

A structural phase transition in $NaTaOGeO_4$ and its relation to phase transitions in titanite

Thomas Malcherek

Mineralogisch-Petrographisches Institut, Universität Hamburg, Grindelallee 48, D-20146 Hamburg, Germany

Correspondence e-mail: thomas.malcherek@uni-hamburg.de

Received 30 January 2007
Accepted 29 May 2007

A structural phase transition from space-group symmetry $P2_1/c$ to $C2/c$ is reported for $NaTaOGeO_4$ (NTGO). The critical temperature has been located at $T_c = 116$ K, based on the appearance of sharp diffraction maxima at positions $h + k = 2n + 1$ of reciprocal space on cooling below this temperature. Strongly anisotropic diffuse scattering in sheets normal to [001] is observable for $T > T_c$ and persists up to ambient temperature. Similarities to phase transitions observed in other compounds of the titanite structure type are discussed. The symmetry properties of these phase transitions are reassessed on the basis of the structural data available. The primary order parameter is identified with the displacement of the transition metal cation M (M = Ta in NTGO) away from the centre of symmetry that it nominally occupies in the paraphase. The order parameter transforms as the Y_2^- representation. The anisotropic diffuse scattering is attributed to the one-dimensional correlation of local M displacements parallel to the direction of chains of *trans*-corner-sharing MO_6 octahedra. The critical temperatures of the isomorphous phase transitions in various titanite-type compounds depend linearly on the squared transition-metal displacement measured in the ordered $P2_1/c$ phase.

1. Introduction

The structure of $NaTaOGeO_4$ (NTGO) was determined and identified with the aristotype structure of titanite by Genkina & Mill (1992). While many synthetic derivatives $AMOXO_4$ of the mineral titanite, $CaTiOSiO_4$, are known, only a few compounds display the distorted low-temperature form of space-group symmetry $P2_1/c$. The distortion is associated with early transition-metal cations occupying the octahedrally coordinated M site. Off-centre displacement of such early transition metals is attributed to the mixing of empty transition-metal d states and the $2p$ states of the oxygen ligands (Kunz & Brown, 1995; Brown, 2002).

In the present article the symmetry properties of the phase transition $P2_1/c \leftrightarrow C2/c$ in titanite are reviewed. The occurrence of an analogous phase transition in NTGO is reported and its properties are compared with those of the other known phase transitions of this kind.

1.1. Symmetry properties

Several synthetic derivatives of titanite, including the title compound, have been described in the conventional space-group settings $C2/c$ or $P2_1/c$ (Mill *et al.*, 1990; Phillips *et al.*, 1992; Genkina & Mill, 1992). A comparison of compounds with the titanite structure type and in particular the comparison of phase transitions occurring in these compounds are hampered by the widespread use of non-conventional space-

group settings for the mineral titanite itself. In the following an attempt is made to reconcile the description of the titanite structure with the standard settings of the relevant space groups.

The first structure determination of titanite by Zachariasen (1930) invoked a cell choice which required the characteristic octahedral chains of the titanite structure to be oriented parallel to [101]. Later on Mongiorgi & Riva di Sanseverino (1968) redetermined the structure in the space-group setting $A2/a$, using a cell on a reduced mesh, *i.e. International Tables* (ITA) cell choice 1. In this setting the octahedral chains are oriented parallel to [100]. For the transformation from $A2/a$ to $C2/c$ the ITA conventions stipulate (Aroyo *et al.*, 2006)

$$\mathbf{P} = \begin{pmatrix} 0 & 0 & 1 \\ 0 & \bar{1} & 0 \\ 1 & 0 & 0 \end{pmatrix}.$$

Hence in $C2/c$ the octahedral chains are oriented parallel to [001]. On the other hand, the ITA setting of $P2_1/a$ would require cell choice 3 and the transformation to $P2_1/c$ with cell choice 1 is obtained by application of the matrix (Aroyo *et al.*, 2006)

$$\mathbf{P}' = \begin{pmatrix} \bar{1} & 0 & \bar{1} \\ 0 & 1 & 0 \\ 1 & 0 & 0 \end{pmatrix}.$$

The structure data available for the transition from $A2/a$ to $P2_1/a$ (Taylor & Brown, 1976; Ghose *et al.*, 1991; Kek *et al.*, 1997) all refer to the identical cell metrics for the low- and high-symmetry phases *i.e.* cell choice 1. Hence the appropriate

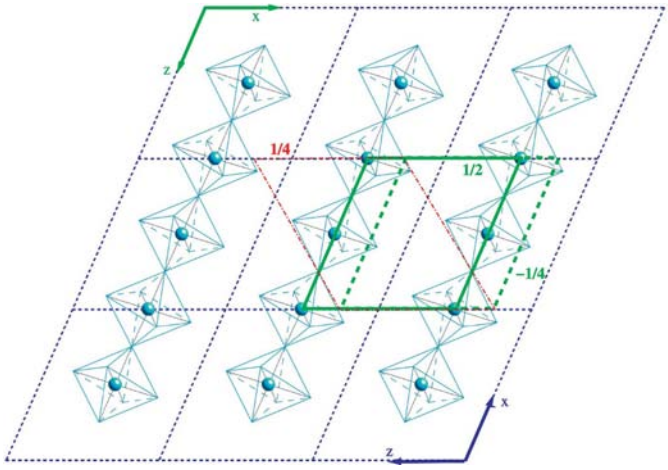

Figure 1
Schematic drawing of unit-cell orientations and shifts relative to the $A2/a$ setting (dashed blue), projected along [010]. Zachariasen's cell choice (dash–dotted red), the cell choice used in this work ($C2/c$, solid green) and the unit cell of the distorted low-temperature phase ($P2_1/c$, dashed green) are shown. Numbers denote the shift parallel to [010] relative to the $A2/a$ setting.

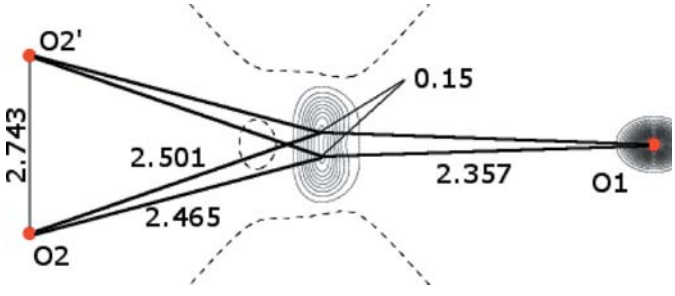

Figure 2
Joint p.d.f. around Na in (100) at ambient temperature. Distances are given in Å. O2 and O2′ are located above and below the plane of projection.

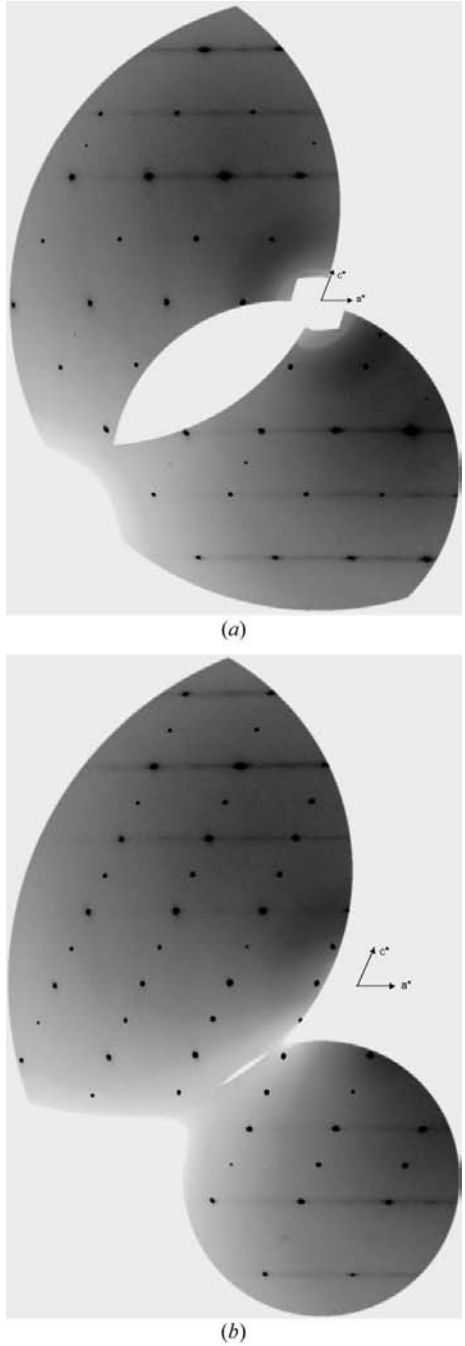

Figure 3
Reconstructed reciprocal space map of (*a*) the *h*0*l* and (*b*) the *h*1*l* layer of NTGO.

Table 1
Experimental and refinement details.

	T_1	T_2
Crystal data		
Chemical formula	$GeNaO_5Ta$	$GeNaO_5Ta$
M_r	356.5	356.5
Cell setting, space group	Monoclinic, $P2_1/c$	Monoclinic, $C2/c$
Temperature (K)	98	295
a, b, c (Å)	6.838 (1), 8.930 (1), 7.414 (1)	6.854 (1), 8.933 (1), 7.418 (1)
β (°)	114.800 (6)	114.858 (2)
V (Å^3)	411.0 (1)	412.10 (9)
Z	4	4
D_x (Mg m^{-3})	5.760	5.745
Radiation type	Synchrotron	Synchrotron
Crystal form, colour	Tabular, colourless	Tabular, colourless
Crystal size (mm^3)	0.1 × 0.09 × 0.045	0.1 × 0.09 × 0.045
Data collection		
Diffractometer	Beamline F1 at Hasylab	Beamline F1 at Hasylab
Data collection method	φ rotation	φ rotation
Absorption correction	None	None
No. of measured, independent and observed reflections	95 016, 20 505, 17 954	95 651, 14 190, 11 959
Criterion for observed reflections	$I > 3\sigma(I)$	$I > 3\sigma(I)$
R_{int}	0.044	0.048
θ_{max} (°)	45.9	53.3
Refinement		
Refinement on	F^2	F^2
$R[F^2 > 3\sigma(F^2)]$, $wR(F^2)$, S	0.023, 0.073, 1.06	0.020, 0.066, 1.02
No. of reflections	20 505	14 190
No. of parameters	74	54
Weighting scheme	Based on measured s.u.'s, $w = 1/[\sigma^2(I) + 0.0016I^2]$	Based on measured s.u.'s, $w = 1/[\sigma^2(I) + 0.0016I^2]$
$(\Delta/\sigma)_{max}$	0.012	0.001
$\Delta\rho_{max}$, $\Delta\rho_{min}$ (e Å^{-3})	2.95, −4.68†	2.59, −2.42
Extinction method	B-C type 1 Gaussian isotropic (Becker & Coppens, 1974)	B-C type 1 Gaussian isotropic (Becker & Coppens, 1974)
Extinction coefficient	0.00345 (16)	0.00728 (19)

Computer programs used: *JANA*2000 (Petricek *et al.*, 2000). † At $x = 0.2618$, $y = 0.2449$, $z = 0.0011$, 0.09 Å from Ta.

transformation for obtaining the cell dimensions of the standard settings $C2/c$ and $P2_1/c$ is **P** in this case. In several descriptions of the titanite aristotype structure, Ti has been placed in the 4(*b*) position (for an example in space-group setting $C2/c$ see Hawthorne *et al.*, 1991). In order to arrive at a description with Ti in 4(*a*) an appropriate unit-cell shift has to be applied. Other permissible translations of $C2/c$, *i.e.* $(\frac{1}{2}, 0, 0)$ and/or $(0, 0, \frac{1}{2})$, may be required to transform other settings of the titanite structure to the one used here. In the final aristotype structure, *i.e.* the setting used by Genkina & Mill (1992), the transition metal *M* occupies the 4(*a*) Wyckoff position, *A*, *X* and one O atom occupy 4(*e*), and the two remaining O atoms are situated on general positions 8(*f*). In the distorted low-temperature structure all atoms occupy a general position. The relative shifts of the various unit-cell definitions are summarized in Fig. 1.

With the above definitions the properties of the transition $P2_1/c \leftrightarrow C2/c$ in titanite have to be reassessed: comparison of the transformed coordinates (Table 2) shows that the irreducible representation of the primary order parameter should be Y_2^-. While Ghose *et al.* (1991) pointed out that Y_2^- involves a pure origin shift by (1/4,1/4,0) (*cf.* also *SYMMODES*; Capillas *et al.*, 2003), the same authors arrived at the conclusion that the low-temperature structure develops according to Y_2^+ instead. However, the resulting space-group symmetry (with respect to the original cell in $C2/c$) would become $P2_1/n$ in this case and the individual displacements would therefore propagate along the [101] direction. As the origin shift is absent for the transformation properties of Y_2^+, Ti would have to remain at the centre of symmetry and only the positions of the other atoms, *i.e.* those occupying the 4(*e*) and 8(*f*) Wyckoff positions, would be affected by the phase transition. It has been suggested that this is the case in the low-temperature structure of $CaTaOAlO_4$ (Malcherek, Borowski & Bosenick, 2004), although a direct experimental confirmation is still missing.

2. Experimental

Single crystals of $NaTaOGeO_4$ were grown following the method described by Mill *et al.* (1990). The obtained small ($V < 0.1$ mm^3) crystals were transparent and colorless. Variable-temperature measurements of crystal (1) for selected areas of reciprocal space between ambient temperature and liquid nitrogen temperature were conducted at ANKA (FZK, Karlsruhe) using a Bruker APEX CCD detector at a wavelength of $\lambda = 0.80078$ Å. These data serve to determine the critical temperature of the phase transition in the following. Diffraction data at constant temperature [crystal (2), $T_1 = 98$ and $T_2 = 295$ K] were collected at Hasylab (DESY, Hamburg) using a 165 mm MARCCD detector at a wavelength of $\lambda = 0.3918$ Å. Owing to the small wavelength, absorption effects were minimized and the data were therefore used for structure determination. Additional ambient temperature data [crystal (1)] were collected at the Swiss–Norwegian beamline (BM1A) of the ESRF facility in Grenoble at a wavelength of $\lambda = 0.710$ Å using a MAR345 image-plate system. Reconstructed reciprocal space images were obtained from these data using the *CrysAlis* software package (Oxford Diffraction, 2004). Data collected with the MARCCD detector at Hasylab were reduced using the *XDS* package (Kabsch, 1993). Crystal structures were refined using *JANA*2000 (Petricek *et al.*, 2000). Anharmonic contributions to the displacements of Na were refined for T_2.

Table 2
Atomic coordinates of the titanite structure at T = 530 K (space group $C2/c$; x, y, z) and at T = 100 K (space group $P2_1/c$; x_1, y_1, z_1) and their relative displacements.

To obtain the coordinates (x_1, y_1, z_1) the transformation matrix **P** and an additional shift of $+(0,0,\frac{1}{2})$ has been applied to the data given by Kek *et al.* (1997).

Atom	x	y	z	$x' = x + 1/4$	$y' = y + 1/4$	$z' = z$
T = 530 K						
Ca	0	0.6690	1/4	1/4	0.9190	1/4
Ti	1/2	1/2	1/2	3/4	3/4	1/2
Si	0	0.3173	1/4	1/4	0.5673	1/4
O1	0	0.9297	1/4	1/4	0.1797	1/4
O2	0.1855	0.4337	0.4114	0.4355	0.6837	0.4114
O2′	0.6855	0.9337	0.4114	0.9355	0.1837	0.4114
O3	0.1035	0.2107	0.1177	0.3535	0.4607	0.1177
O3′	0.6035	0.7107	0.1177	0.8535	0.9607	0.1177

Atom	x_1	y_1	z_1
T = 100 K			
Ca	0.25115	0.91845	0.2410
Ti	0.74926	0.75456	0.5149
Si	0.24877	0.5672	0.2480
O1	0.2502	0.1793	0.2505
O2a	0.4349	0.6843	0.4105
O2b	0.9378	0.1847	0.4134
O3a	0.3534	0.4610	0.1161
O3b	0.8535	0.9598	0.1185

Atom	$\delta_x = x_1 - x'$	$\delta_y = y_1 - y'$	$\delta_z = z_1 - z'$
Displacements			
Ca	0.00115	−0.00055	−0.009
Ti	−0.00074	0.00456	0.0149
Si	−0.00123	−0.0001	−0.002
O1	0.0002	−0.0004	0.0005
O2	−0.0005	0.0007	−0.0010
O3	0.0028	0.0011	0.0020
O4	−0.0001	0.0003	−0.0016
O5	0.0	−0.0009	0.0008

Table 3
Atomic coordinates of NTGO at T = 295 and 98 K and the relative static displacements δ_x, δ_y, δ_z.

For T = 295 K the (1/4,1/4,0) shift has been applied and atoms related by the base centering have been listed seperately, in order to emphasize the relation to the distorted structure.

Atom	$x + 1/4$	$y + 1/4$	z	U_{eq}
T = 295 K, space group $C2/c$				
Na	1/4	0.9241 (1)	1/4	0.0200 (2)
Ta	3/4	3/4	1/2	0.00684 (1)
Ge	1/4	0.56758 (1)	1/4	0.00632 (1)
O1	1/4	0.1837 (1)	1/4	0.0094 (1)
O2	0.4458 (1)	0.6883 (1)	0.4112 (1)	0.0114 (1)
O2′	0.9458 (1)	0.1883 (1)	0.4112 (1)	0.0114 (1)
O3	0.3477 (1)	0.4553 (1)	0.1124 (1)	0.0100 (1)
O3′	0.8477 (1)	0.9553 (1)	0.1124 (1)	0.0100 (1)

Atom	x_1	y_1	z_1	U_{eq}
T = 98 K, space group $P2_1/c$				
Na	0.24827 (4)	0.92207 (6)	0.24235 (5)	0.0111 (1)
Ta	0.748245 (2)	0.752060 (2)	0.504007 (3)	0.003180 (5)
Ge	0.249340 (6)	0.567282 (8)	0.249414 (6)	0.003072 (8)
O1	0.25058 (5)	0.18307 (5)	0.24884 (4)	0.00508 (5)
O2	0.44387 (6)	0.68888 (4)	0.41119 (6)	0.00602 (5)
O3	0.94724 (6)	0.18710 (4)	0.41330 (6)	0.00594 (5)
O4	0.35039 (6)	0.45542 (4)	0.11373 (6)	0.00544 (5)
O5	0.84765 (6)	0.95470 (4)	0.11214 (6)	0.00540 (5)

Atom	δ_x	δ_y	δ_z
Displacements			
Na	−0.00173	−0.00203	−0.00765
Ta	−0.00175	0.00206	0.004
Ge	−0.00066	−0.00023	−0.00059
O1	0.0006	−0.0006	−0.0012
O2	−0.0019	0.0006	0.0
O3	0.0014	−0.0012	0.0021
O4	0.0027	0.0001	−0.0013
O5	−0.0001	−0.0006	−0.0003

3. Results and discussion

Measurement and refinement details for NTGO are summarized in Table 1.[1] The structural data obtained for the two polymorphs are compared in Table 3. Harmonic and anharmonic contributions to the temperature movements are listed in Tables 4 and 5, respectively. The positional parameters at room temperature agree well with the data determined by Genkina & Mill (1992).

Calculation of the bond-valence sums (BVS) with parameters of Brese & O'Keeffe (1991) shows ideal values for Na, Ge, O2 and O3 in the low- and ambient-temperature phases. Ta and O1 are both overbonded with a BVS of 5.12 and 2.1, respectively. Similar overbonding of Ti and O1 does occur in titanite.

The probability density function (p.d.f.) of Na at room temperature is shown in Fig. 2. It indicates site disorder of the A cation similar to $LiTaOGeO_4$ (LTGO; Malcherek, 2002). The two positions of Na are 0.15 Å apart, which amounts to only about half the distance observed for Li in LTGO. Owing to resolution limits the p.d.f. appears rather flat and it is not possible to derive a significant barrier height from the associated one-particle potential. The reconstructed reciprocal space images of NTGO (Fig. 3) at ambient temperature exhibit anisotropic thermal diffuse scattering in sheets normal to [001] with $l = 2n$. Similar sheets of diffuse scattering have been observed in $LiTaOGeO_4$, $CaTiOGeO_4$ and titanite. Some weak but very sharp reflections with $l = 2n + 1$, *e.g.* $00\bar{5}$ or $\bar{2}05$, are visible in the $h0l$ layer of Fig. 3. These apparent violations of the c-glide symmetry operation are likely to be caused by multiple diffraction effects, as no significant systematic absence violations have been observed in the data used for structure refinement. Fig. 4 shows the squared intensity ratio of the superstructure reflections $01\bar{6}$ and $12\bar{6}$, and the fundamental reflection $\bar{2}\bar{2}\bar{5}$ as a function of the temperature. A linear fit to these data yields an extrapolated critical temperature of T_c = 115.8 (6) K. The linear temperature dependence of the squared intensity of the superstructure reflections is in agreement with the behaviour of other compounds of this type (Malcherek, Bosenick *et al.*, 2004). As

[1] Supplementary data for this paper are available from the IUCr electronic archives (Reference: CK5025). Services for accessing these data are described at the back of the journal.

Table 4
Harmonic temperature parameters (Å^2) at T = 295 and 98 K.

The correction factor for the harmonic contributions takes the form $\exp[2\pi^2(U^{11}h^2a^{*2} + U^{22}h^2b^{*2} + U^{33}h^2c^{*2} + U^{12}hka^*b^* + U^{13}hla^*c^* + U^{23}klb^*c^*)]$.

Atom	U^{11}	U^{22}	U^{33}	U^{12}	U^{13}	U^{23}
T = 295 K, space group $C2/c$						
Na	0.0153 (3)	0.0127 (3)	0.0282 (4)	0	0.0053 (3)	0
Ta	0.006618 (6)	0.006617 (7)	0.006871 (7)	0.000740 (2)	0.002422 (4)	−0.000577 (3)
Ge	0.00604 (1)	0.00585 (1)	0.00668 (1)	0	0.00230 (1)	0
O1	0.0131 (1)	0.0097 (1)	0.0061 (1)	0	0.0047 (1)	0
O2	0.0082 (1)	0.0122 (1)	0.0128 (1)	−0.0033 (1)	0.0033 (1)	−0.0037 (1)
O3	0.0123 (1)	0.0076 (1)	0.0123 (1)	−0.0012 (1)	0.0072 (1)	−0.0027 (1)
T = 98 K, space group $P2_1/c$						
Na	0.00875 (12)	0.00526 (9)	0.01730 (19)	−0.00006 (5)	0.00358 (12)	−0.00022 (7)
Ta	0.002967 (6)	0.003137 (6)	0.003265 (7)	−0.000264 (2)	0.001138 (5)	0.000239 (2)
Ge	0.00288 (1)	0.00298 (1)	0.00323 (1)	0.00001 (1)	0.00115 (1)	−0.00001 (1)
O1	0.00648 (8)	0.00553 (8)	0.00360 (6)	0.00003 (4)	0.00248 (6)	0.00003 (5)
O2	0.00439 (7)	0.00633 (8)	0.00681 (8)	−0.00152 (6)	0.00183 (6)	−0.00164 (7)
O3	0.00457 (7)	0.00619 (8)	0.00663 (8)	−0.00150 (6)	0.00192 (6)	−0.00151 (7)
O4	0.00622 (7)	0.00451 (7)	0.00654 (8)	−0.00052 (5)	0.00360 (6)	−0.00135 (6)
O5	0.00621 (7)	0.00440 (6)	0.00646 (8)	−0.00048 (5)	0.00351 (6)	−0.00122 (6)

in titanite (Malcherek *et al.*, 2001), the superstructure reflections remain visible immediately above T_c in the form of diffuse intensity maxima that are superimposed onto the diffuse sheets in layers of $l = 2n$.

Comparison of the static displacements in titanite and in NTGO (Tables 2 and 3) shows that the largest displacements have equal direction for both compounds. Having the smaller critical temperature, the overall displacements in NTGO are evidently smaller as well, as will be further discussed below. However, the z component of the Ta displacement is less pronounced than the corresponding Ti displacement component. While the δ_x/δ_z ratio of the M displacement in titanite is only −0.04, it amounts to −0.44 in NTGO. A similar rotation of the short Ta—O1 bond away from the position of the average bond in the paraphase is known for the phase transition in LTGO (Malcherek, 2002). While the resulting sublattice polarization is nearly parallel to [001] in titanite, it deviates from this direction within the (010) plane in NTGO and LTGO.

In titanite the static Ca displacement is significantly smaller than the Ti displacement. In NTGO the corresponding displacement of Na is almost as large as that of Ca in titanite and its z component is in fact larger than the z component of the Ta displacement. At the same time the x and y components of Na and Ta displacement are nearly identical but of opposite sign in NTGO. The A cation is generally expected to be disordered above T_c across a split position that is characteristic of the intermediate phase (Kek *et al.*, 1997). Therefore, its displacement would not occur at T_c, but the A atoms would

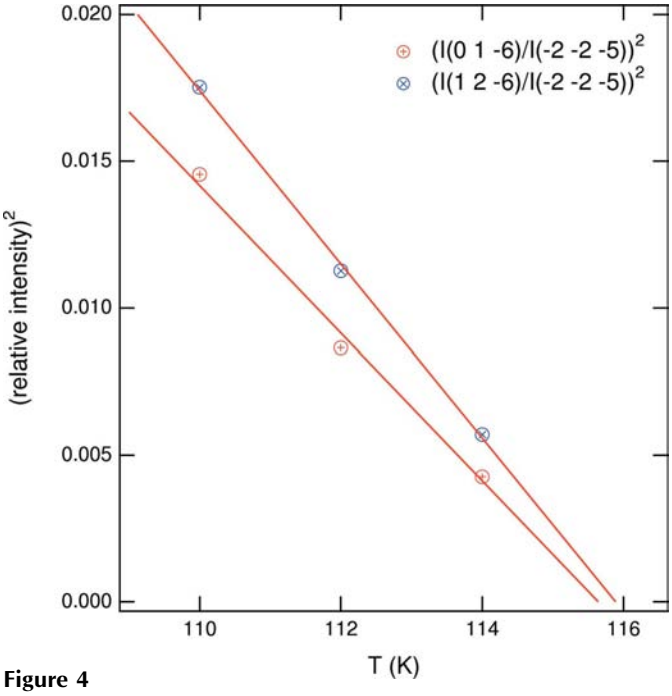

Figure 4
Squared relative intensity of two superstructure reflections as a function of temperature. Straight-line fits have been used to extrapolate T_c.

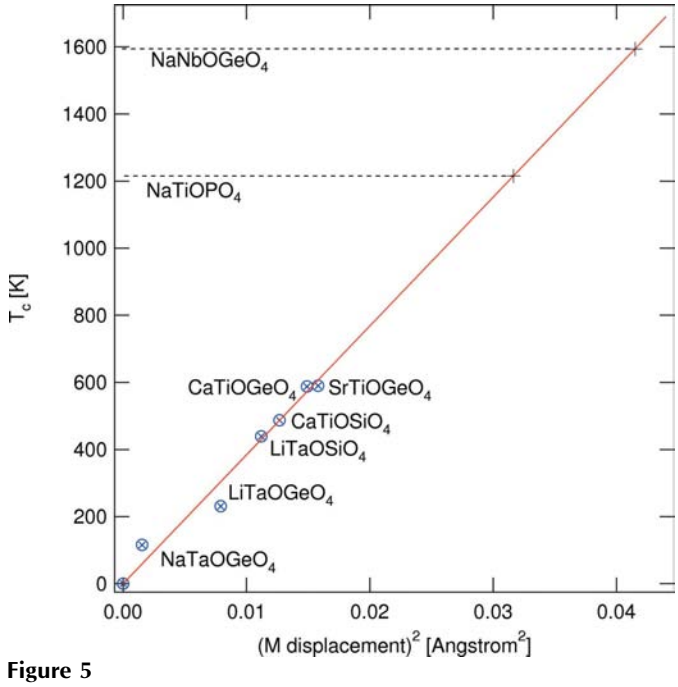

Figure 5
T_c as a function of the squared-static transition-metal cation displacement. The line has been constrained to pass the origin. Structure data and critical temperatures have been obtained from Kek *et al.* (1997) (titanite), Malcherek (2002) ($LiTaOGeO_4$), Genkina & Mill (1992), Malcherek, Bosenick *et al.* (2004) ($LiTaOSiO_4$), Ellemann-Olesen & Malcherek (2005*a*) ($CaTiOGeO_4$) and Ellemann-Olesen & Malcherek (2005*b*) ($SrTiOGeO_4$). Extrapolated values of T_c for α-$NaTiOPO_4$ and $NaNbOGeO_4$ have been obtained using the known structure data of the respective distorted phases (Phillips *et al.*, 1992; Mill *et al.*, 1990).

Table 5
Third- and fourth-order tensorial coefficients γ_{ijk} ($\times$1000) and δ_{ijkl} ($\times$1000) for Na at T = 295 K.

The correction factor for the anharmonic contributions takes the form $\left[1 - i\frac{4}{3}\pi^3(h^3\gamma_{111} + k^3\gamma_{222} + \ldots + hl^2\gamma_{233} + hkl\gamma_{123}) + \frac{2}{3}\pi^4(h^4\delta_{1111} + k^4\delta_{2222} + \ldots + k^2l^2\delta_{2233} + kl^3\delta_{2333})\right]$.

	γ_{222}	γ_{112}	γ_{233}	γ_{123}					
Na	−0.93 (8)	−1.09 (9)	0.3 (1)	0.0 (1)					
	δ_{1111}	δ_{2222}	δ_{3333}	δ_{1113}	δ_{1122}	δ_{1133}	δ_{1223}	δ_{1333}	δ_{2233}
Na	−1.50 (9)	0.08 (3)	−5.9 (3)	−0.74 (7)	−0.08 (2)	−0.61 (8)	0.04 (2)	−0.46 (12)	0.08 (4)

rather start to order onto one of the displaced positions at this temperature.

Fig. 5 demonstrates that the critical temperature follows the Abrahams–Kurtz–Jamieson law (Abrahams *et al.*, 1968) if the transition metal displacement is defined by the distance to the (appropriately transformed) 4(*a*) position of the space group *C*2/*c*. The static displacements have been obtained using the published structural data of various compounds occurring in the distorted titanite structure. The Ta displacement of NTGO is apparently smaller than expected from the obtained linear relationship between squared *M* cation displacement and critical temperature. This particular deviation may be due to the relatively large reduced temperature, T/T_c = 0.845, at which the low-temperature structure reported here has been determined. Structure determination at lower temperatures might attain a more saturated order parameter and consequently a slightly larger Ta displacement. Using the derived linear relationship it is possible to estimate the stability of the distorted phase as a function of composition for compounds that have the titanite topology in common. Compounds with *M* = Ta generally have the lowest T_c. A strikingly large difference of 1500 K exists between T_c in $NaTaOGeO_4$ and the extrapolated T_c of $NaNbOGeO_4$. $NaNbOGeO_4$ decomposes at $\sim$1373 K (Mill *et al.*, 1990), hence the phase transition cannot be observed under ambient pressure conditions in this compound. The larger off-centre distortion in $NaNbOGeO_4$ and the related higher stability of the $P2_1/c$ structure has to be attributed to the electronic configuration of the transition metal, as the radii of Ta^{5+} and Nb^{5+} are indistinguishable. Similar, albeit smaller, differences of the critical temperatures and of the related distortions are known to occur in various oxide ferroelectrics, *e.g.* the pairs $LiNbO_3/LiTaO_3$ or $KNbO_3/KTaO_3$, where the latter compound is commonly described as incipient ferroelectric (*e.g.* Akbarzadeh *et al.*, 2004). Possible reasons for the different behaviour of the 4*d* and 5*d* systems have been discussed by Kaupp (2001).

G. Buth and C. Paulmann are thanked for their support during the measurements at ANKA and at Hasylab respectively. The author also wishes to thank U. Bismayer and M. Aroyo for helpful discussions. Financial support by the Deutsche Forschungsgemeinschaft is gratefully acknowledged.

References

Abrahams, S. C., Kurtz, S. K. & Jamieson, P. B. (1968). *Phys. Rev.* **172**, 551–553.
Akbarzadeh, A. R., Bellaiche, L., Leung, K., Iniguez, J. & Vanderbilt, D. (2004). *Phys. Rev. B*, **70**, 054103.
Aroyo, M. I., Perez-Mato, J. M., Capillas, C., Kroumova, E., Ivantchev, S., Madariaga, G., Kirov, A. & Wondratschek, H. (2006). *Z. Kristallogr.* **221**, 15–27.
Becker, P. J. & Coppens, P. (1974). *Acta Cryst.* A**30**, 129–153.
Brese, N. E. & O'Keeffe, M. (1991). *Acta Cryst.* B**47**, 192–197.
Brown, I. D. (2002). *The Chemical Bond in Inorganic Chemistry*. Oxford University Press.
Capillas, C., Kroumova, E., Aroyo, M. I., Perez-Mato, J. M., Stokes, H. T. & Hatch, D. M. (2003). *J. Appl. Cryst.* **36**, 953–954.
Ellemann-Olesen, R. & Malcherek, T. (2005*a*). *Am. Mineral.* **90**, 1325–1334.
Ellemann-Olesen, R. & Malcherek, T. (2005*b*). *Phys. Chem. Miner.* **32**, 531–545.
Genkina, E. A. & Mill, B. V. (1992). *Sov. Phys. Crystallogr.* **37**, 769–772.
Ghose, S., Ito, Y. & Hatch, D. M. (1991). *Phys. Chem. Miner.* **17**, 591–603.
Hawthorne, F., Groat, L., Raudsepp, M., Ball, N., Kimata, M., Spike, F., Gaba, R., Halden, N., Lumpkin, G., Ewing, R., Greegor, R., Lytle, F., Ercit, T., Rossman, G., Wicks, F., Ramik, R., Sherriff, B., Fleet, M. & McCammon, C. (1991). *Am. Mineral.* **76**, 370–396.
Kabsch, W. (1993). *J. Appl. Cryst.* **26**, 795–800.
Kek, S., Aroyo, M., Bismayer, U., Schmidt, C., Eichhorn, K. & Krane, H. (1997). *Z. Kristallogr.* **212**, 9–19.
Kaupp, M. (2001). *Angew. Chem. Int. Ed.* **40**, 3534–3565.
Kunz, M. & Brown, I. D. (1995). *J. Solid State Chem.* **115**, 395–406.
Malcherek, T. (2002). *Acta Cryst.* B**58**, 607–612.
Malcherek, T., Borowski, M. & Bosenick, A. (2004). *J. Appl. Cryst.* **37**, 117–122.
Malcherek, T., Bosenick, A., Cemič, L., Fechtelkord, M. & Guttzeit, A. (2004). *J. Solid State Chem.* **177**, 3254–3262.
Malcherek, T., Paulmann, C., Domeneghetti, M. C. & Bismayer, U. (2001). *J. Appl. Cryst.* **34**, 108–113.
Mill, B., Belokoneva, E. & Butashin, A. (1990). *Sov. Phys. Crystallogr.* **35**, 176–180.
Mongiorgi, R. & Riva di Sanseverino, L. (1968). *Miner. Petrogr. Acta*, **14**, 123–141.
Oxford Diffraction (2004). *CrysAlis*. Oxford Diffraction, Abingdon, Oxfordshire, UK.
Petricek, V., Dusek, M. & Palatinus, L. (2000). *JANA*2000. Institute of Physics, Praha, Czech Republic.
Phillips, M. L. F., Harrison, W. T. A., Stucky, G. D., McCarron III, E. M., Calabrese, J. C. & Gier, T. E. (1992). *Chem. Mater.* **4**, 222–233.
Taylor, M. & Brown, G. E. (1976). *Am. Mineral.* **61**, 435–447.
Zachariasen, W. H. (1930). *Z. Kristallogr.* **73**, 7–16.